Estimation of Paclitaxel Biodistribution and Uptake in Human-Derived Xenografts In Vivo with ^{18}F-Fluoropaclitaxel

Anne Gangloff, PhD[1]*; Wei-Ann Hsueh, BS[1]*; Amanda L. Kesner, PhD[1]; Dale O. Kiesewetter, PhD[2]; Betty S. Pio, MSc[1]; Mark D. Pegram, MD[3]; Malgorzata Beryt, MSc[3]; Allison Townsend, BS[1]; Johannes Czernin, MD[1]; Michael E. Phelps, PhD[1]; and Daniel H.S. Silverman, MD, PhD[1]

[1]Ahmanson Biological Imaging Division, Department of Molecular and Medical Pharmacology, David Geffen School of Medicine, University of California, Los Angeles, California; [2]Warren Grant Magnuson Clinical Center, National Institutes of Health, Bethesda, Maryland; and [3]Divison of Hematology and Oncology, Department of Medicine, David Geffen School of Medicine, University of California, Los Angeles, California

Paclitaxel (PAC) is widely used as a chemotherapy drug in the treatment of various malignancies, including breast, ovarian, and lung cancers. We examined the biodistribution of ^{18}F-fluoropaclitaxel (^{18}F-FPAC) in mice with and without human breast cancer tumor xenografts by use of small-animal–dedicated PET (microPET) and clinically practical semiquantitative methods. We compared the PET data to data derived from direct harvesting and analysis of blood, organs, and breast carcinoma xenografts. **Methods:** PET data were acquired after tail vein injection of ^{18}F-FPAC in nude mice. Tracer biodistribution in reconstructed images was quantified by region-of-interest analysis. Biodistribution also was assessed by harvesting and analysis of dissected organs, tumors, and blood after coadministration of ^{18}F-FPAC and ^{3}H-PAC. ^{18}F content in each tissue was assessed with a γ-well counter, and ^{3}H content was quantified by scintillation counting of solubilized tissue after ^{18}F radioactive decay. **Results:** The distributions of ^{18}F-FPAC and ^{3}H-PAC were very similar, with the highest concentrations in the small intestine, the lowest concentrations in the brain, and intermediate concentrations in tumor. Uptake in these and other tissues was not inhibited by the presence of more pharmacologic doses of unlabeled PAC. Administration of the P-glycoprotein modulator cyclosporine doubled the uptake of both ^{18}F-FPAC and ^{3}H-PAC into tumor. **Conclusion:** PET studies with ^{18}F-FPAC can be used in conjunction with clinically practical quantification methods to yield estimates of PAC uptake in breast cancer tumors and normal organs noninvasively.

Key Words: breast cancer; paclitaxel; ^{18}F; PET; microPET

J Nucl Med 2005; 46:1866–1871

Breast cancer is the second leading cause of death among cancers in women (*1*). Chemotherapy is commonly used in the treatment of breast cancer in neoadjuvant, adjuvant, and metastatic therapy settings. A substantial portion of tumors will fail to respond, however, and no generally reliable tool for predicting the outcome of chemotherapy treatment is clinically available to date. Accurate predictors of the response to chemotherapy in individuals with cancer clearly would be valuable for guiding optimal clinical management. Currently, the selection of therapeutic regimens with chemotherapy agents is based on a few parameters (e.g., tumor histology, clinical stage, erb-B2 (Her2/neu) and estrogen receptor status, and history of prior therapy), and effectiveness remains variable from patient to patient. This situation results in some patients receiving highly toxic drugs from which they fail to benefit and possible delays in receiving regimens from which they might benefit the most. A significant obstacle to improving this situation has been that prediction models designed to test chemotherapy agents against tumor cell lines or biopsy specimens in vitro have been unsuccessful in identifying many cases of resistance to those agents in vivo. We have hypothesized that this lack of predictive power relates largely to the pharmacokinetics of the drugs combined with local environmental factors of the tumors that are not recapitulated in vitro but could potentially be quantified in vivo by imaging-based methods.

Rates of responses of various human tumor types to conventional cytotoxic chemotherapeutic drugs historically have been empirically derived by treating a cohort of patients having a particular type of cancer with a given chemotherapeutic regimen and observing the proportion of responding patients. Individual responses vary substantially, however, from complete remission to disease progression. For this reason, attempts have been made to individualize treatment by studying the responses of the patients' biopsied tumor cells to cytotoxic chemotherapeutic drugs in vitro (*2–11*). In general, these assay systems have a reasonable negative predictive value, predicting resistance to various chemotherapeutic agents, but no assay system has yet been found to have an accurate positive predictive value—that is, predicting sensitivity to those drugs in vivo. This situation is

Received Apr. 26, 2005; revision accepted Aug. 2, 2005.
For correspondence or reprints contact: Daniel H.S. Silverman, MD, PhD, CHS AR-144, Nuclear Medicine Clinic, MC694215, UCLA Medical Center, Los Angeles, CA 90095-6942.
E-mail: dsilver@ucla.edu
*Contributed equally to this work.
Guest Editor: John A. Katzenellenbogen

perhaps not surprising, as the tumoral environment in vivo, which affects the disposition of chemotherapeutic drugs, cannot be adequately replicated in vitro.

Several studies have aimed to develop radiolabeled chemotherapy tracers to study noninvasively the uptake of chemotherapy agents in vivo. Li et al. demonstrated the use of ^{111}In-diethylenetriaminepentaacetic acid-paclitaxel as an imaging agent in mammary tumors (*12*). Tracers such as 5-^{18}F-fluorouracil (^{18}F-FU) and acridine derivative ^{11}C-*N*-[2-(dimethylamino)ethyl]acridine-4-carboxamide have been studied as potential PET tracers to predict responses to treatment with fluorouracil and amsacrine for gastrointestinal and acute myelogenous leukemias, respectively (*13*). Paclitaxel (PAC) is a naturally occurring compound with antitumor activity that inhibits cellular proliferation through the stabilization of tubulin (*14*). In order to study taxane biodistribution in vivo, a synthetic scheme to make ^{18}F-fluoropaclitaxel (^{18}F-FPAC) was previously developed. It was shown that the amide side group of PAC can be fluorinated without substantial alteration of its pharmacokinetic properties (*15–17*), and conventionally determined biodistribution of the tracer in healthy mice was reported recently (*16*). In the present study, we first verified that the distribution of the tracer observed in the current model (female athymic mice bearing human breast cancer xenografts and injected with PAC in dimethyl sulfoxide [DMSO] vehicle) was similar to the distribution previously described in a healthy mouse model. Second, we examined the feasibility of using PET to estimate noninvasively the uptake of PAC in tumor as well as normal organs by quantification methods that are sufficiently straightforward to have ready translational potential for the clinical arena.

MATERIALS AND METHODS

Materials

Unless otherwise noted, all chemicals were purchased from Sigma-Aldrich or Fisher Scientific and were of the highest grade available. MCF-7 cells (American Type Culture Collection) were propagated for use in RPMI medium (Invitrogen) supplemented with 10% fetal bovine serum (Invitrogen), L-glutamine at 2 mmol/L (Invitrogen), and 1% penicillin–streptomycin (Invitrogen). All cell lines were maintained in a humidified 37°C 5% CO_2 environment.

Radiosynthesis of ^{18}F-FPAC

The radiosynthesis of ^{18}F-FPAC was performed with method B described by Kiesewetter et al. (*15*). The synthesis included 2 steps: nucleophilic aromatic substitution by ^{18}F-fluoride on pentamethylbenzyl trimethylammoniumbenzoate followed by hydrolysis with trifluoroacetic acid to form ^{18}F-fluorobenzoic acid and treatment of ^{18}F-fluorobenzoic acid and 3′-debenzoyl PAC with diethyl cyanophosphonate and triethylamine, resulting in amide formation to the desired ^{18}F-FPAC. Total synthesis time ranged between 90 and 120 min, with a radiochemical yield of approximately 10% and a purity of ≥97%. Specific activity ranged between 3.7×10^{11} and 1.1×10^{12} Bq/mmol (10 and 30 Ci/mmol).

Breast Cancer Xenografts in Nude Mice

All animal studies were performed under a protocol approved by the Chancellor's Animal Research Committee of UCLA. MCF-7 cells, which form xenografts in athymic mice, were injected subcutaneously at $\sim 3.0 \times 10^7$ cells per tumor into the shoulder region of 4- to 6-wk-old female athymic mice weighing 20–30 g (Charles River Laboratories, Inc.). Before cell injection, all mice were primed with 17β-estradiol (Innovative Research of America) applied subcutaneously (1.7 mg of estradiol per pellet) to promote tumor growth.

Biodistribution of ^{18}F-FPAC

A 100-μL solution containing ~9 MBq of ^{18}F-FPAC and 0.12 MBq of ^{3}H-PAC (35 Ci/mmol), with or without unlabeled PAC (Acros Organics USA) at 20 mg/kg, in vehicle was injected via the tail vein into female nude mice (CD-1 *nu/nu*; Charles River Laboratories, Inc.), some bearing MCF-7 human breast cancer tumor xenografts. The first 32 animals were injected with ^{18}F-FPAC dissolved in ethanol, as in previous work with ungrafted mice having intact immune systems. In nude mice, symptoms characteristic of ethanol toxicity (aggressive behavior, neurologic effects, and acute hyperthermia followed by hypothermia) were observed frequently, and 4 of 32 mice died shortly afterward. In subsequent studies, we used ^{18}F-FPAC dissolved in DMSO and observed a comparable biodistribution but no evident toxicity.

Mice were anesthetized by inhalation of 2% isofluorane, and 5-min scans were acquired after 30 min of uptake by use of a Concorde P4 microPET instrument (Concorde Microsystems Inc.) with the mouse in the prone position and the long axis of the mouse set parallel to the plane of the detectors. Mice were sacrificed immediately after the end of the scan by intracardiac administration of pentobarbital sodium. Organs were harvested and weighed. γ-Counting was done to assess the radioactivity concentration in each tissue, and the percentage injected dose per gram (%ID/g) of tissue was calculated. After all ^{18}F decayed, organs were dissolved in Solvable (Perkin–Elmer Life Sciences) according to the supplier's specifications, and Hionic-Fluor scintillation cocktail (Packard) was added for β-counting. In order to provide a unit most directly analogous to the most commonly used imaging unit in clinical settings, data were expressed as harvested standardized uptake values (hSUVs), corresponding to the measured radioactivity per gram in a given organ divided by the average radioactivity per gram in all harvested organs. All microPET images were reconstructed, and regional tracer concentrations were quantified by use of ASIPRO (Concorde Microsystems Inc.) and CAPP (Research Systems, Inc.) software packages. Quantitative data were expressed as measured standardized uptake values (mSUVs), defined as region-of-interest counts per second per pixel divided by total body counts per second per pixel. Biodistribution and uptake data under different conditions were compared by use of unpaired, 2-tailed Student *t* tests, and significance of correlations was assessed by use of 1-sample *t* tests of the associated Pearson coefficients.

Biodistribution of ^{18}F-FPAC After Pretreatment of Mice with Cyclosporine

Mice bearing MCF-7 tumors were pretreated intraperitoneally with cyclosporine (Novartis Pharmaceuticals) at 0 or 10 mg/kg. After 4 h, the mice were given ^{18}F-FPAC and ^{3}H-PAC in DMSO. All mice underwent microPET imaging, and organs were harvested and processed as described above.

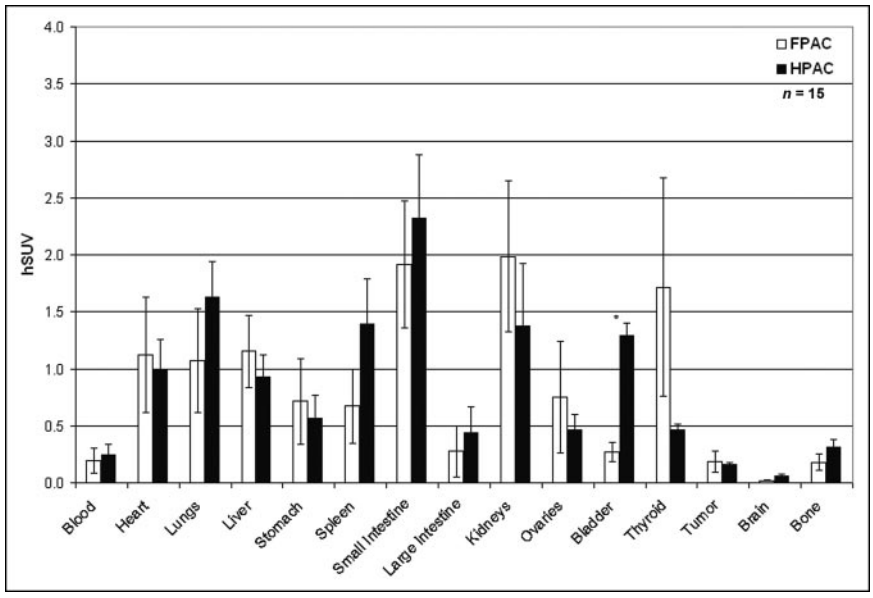

FIGURE 1. Comparison of biodistributions of ^{18}F-FPAC and ^{3}H-PAC in MCF-7 tumor–bearing nude mice 35 min after injection of ^{18}F-FPAC. Values are mean ± SEM. *$P < 0.05$.

RESULTS

It was recently established that ^{18}F-FPAC exhibits biodistribution properties very similar to those of PAC (*16,17*). To verify that ^{18}F-FPAC biodistribution accurately reflected PAC biodistribution in the current animal model, mice were coinjected with ^{18}F-FPAC and ^{3}H-PAC, and the relative biodistributions were compared. The relative biodistributions of ^{18}F-FPAC and ^{3}H-PAC tracers in female nude mice bearing MCF-7 tumors were very similar, except in the bladder (Fig. 1). The organs of greatest concentration were related to excretory pathways (mean ± SEM ^{18}F-FPAC hSUV in the liver, 1.2 ± 0.3; mean ± SEM hSUV in the small intestine, 1.9 ± 0.6; mean ± SEM hSUV in the kidneys, 2.0 ± 0.7). Very little ^{18}F-FPAC was found in the brain (mean ± SEM hSUV, 0.02 ± 0.01), consistent with the known presence of a P-glycoprotein (P-gp) exporter at the blood–brain barrier. Tumor uptake of ^{18}F-FPAC was variable, but hSUVs were in the ranges seen for other soft tissues (mean ± SEM hSUV in tumor, 0.2 ± 0.09). These findings are consistent with what has been reported in previous literature on the biodistribution of PAC analogs in tumor-bearing murine models (*18*).

As the amount of tracer injected was about 2 orders of magnitude lower than the dose typically used to treat mice bearing these xenografts in our murine models, it was relevant to examine whether the behavior of the tracer was altered by the presence of a more pharmacologic dose of unlabeled PAC (Fig. 2). The uptake of ^{18}F-FPAC was not significantly altered in tumor or in any of the organs examined.

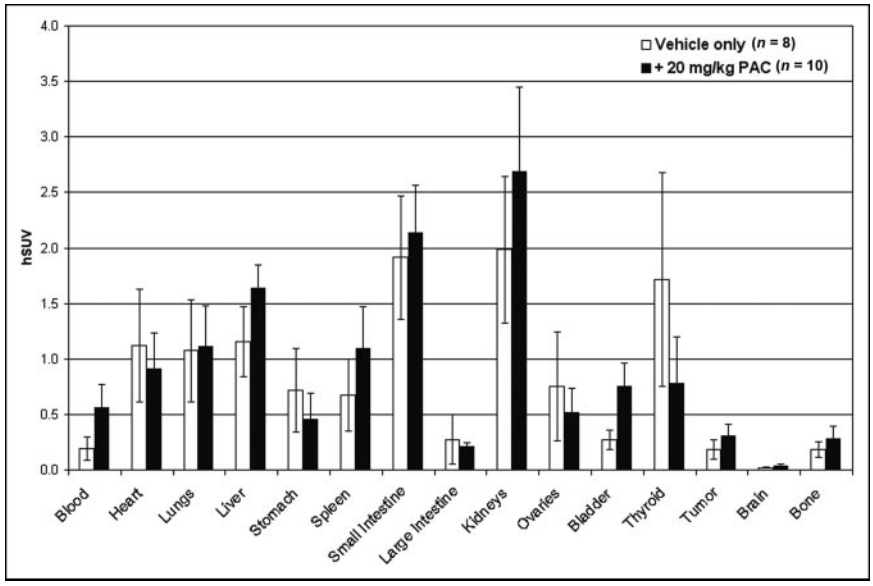

FIGURE 2. Comparison of ^{18}F-FPAC biodistribution in MCF-7 tumor–bearing nude mice 35 min after injection of ^{18}F-FPAC in presence and absence of unlabeled PAC. Values are mean ± SEM.

TABLE 1
Tumor Uptake of ^{3}H-PAC and ^{18}F-FPAC in Presence and Absence of P-gp Modulator Cyclosporine 35 Minutes After Injection

Tracer	Cyclosporine (mg/kg)	Mean hSUV	SEM
^{3}H-PAC	0	0.15	0.02
^{3}H-PAC	10	0.31	0.07*
^{18}F-FPAC	0	0.05	0.01
^{18}F-FPAC	10	0.11	0.03*

*Nonsignificant trend was observed for increase in tumor uptake of each tracer in presence of cyclosporine ($P \leq 0.10$).

The uptake of ^{18}F-FPAC also was determined in the presence or absence of cyclosporine, an inhibitor of the P-gp efflux pump (*19*), in 8 mice, because PAC is a known substrate for P-gp (*20*). As previously shown for the effect of cyclosporine on ^{18}F-FPAC (*17*), the brain showed only a trend toward a modest increase (from an hSUV of 0.0046 ± 0.0011 to an hSUV of 0.0063 ± 0.0015) with cyclosporine treatment, whereas more significant increases were seen in the liver and lungs (from an hSUV of 1.15 ± 0.18 to an hSUV of 1.79 ± 0.17 and from an hSUV of 0.13 ± 0.049 to an hSUV of 0.50 ± 0.084, respectively). Tumor uptake of both ^{3}H-PAC and ^{18}F-FPAC was similarly affected by the presence of cyclosporine at 10 mg/kg (Table 1).

microPET imaging data yielded results similar to those obtained from the harvested tissue data. Tracer distribution was strongly related to routes of metabolism and excretion. Accumulation in the liver (mean ± SEM mSUV, 3.97 ± 0.40) and kidneys (mean ± SEM mSUV, 1.94 ± 0.17) was relatively high. The brain accumulated very little or no tracer (mean ± SEM mSUV, 0.07 ± 0.01), whereas tumor uptake was intermediate (mean ± SEM mSUV, 0.25 ± 0.28) (Figs. 3 and 4).

Because the conventionally used uptake unit, %ID/g, includes tracer activity that is not fully systemically mobilized, we used hSUVs (see Materials and Methods), which normalize tumor and organ contents for this problem. We compared the performance of the hSUV unit described here with the more traditionally used %ID/g unit. There was a strong correlation across organs between the values expressed in these 2 types of units ($r = 0.97$, $P = 0.004$) (Fig. 5). However, for tumor and most organs (liver, kidneys, lungs, and heart), the standard deviations reflected greater interanimal data scatter with the traditionally used %ID/g unit than with the hSUV unit. Also, compared with image-based mSUVs, harvested activity expressed as hSUVs was somewhat better correlated ($r = 0.84$, $P = 0.02$) than activity expressed as %ID/g values ($r = 0.71$, $P = 0.07$) when values for each organ in 22 mice were examined. In addition, when data generated on an individual-animal basis were examined, mSUVs were more strongly correlated with hSUVs ($r = 0.41$, $P < 0.0001$, $n = 154$) than with %ID/g values ($r = 0.25$, $P = 0.002$, $n = 154$).

DISCUSSION

Although ^{18}F-FDG has been by far the most extensively used radiopharmaceutical for oncologic nuclear imaging with PET, the development of several new radiopharmaceutical agents has made it possible to monitor a variety of biologic processes pertinent to the diagnosis and treatment of cancer (*21*). This technology, however, is only now beginning to be applied to the problem of systematically guiding the initial selection of therapy for patients with a given diagnosis. The feasibility of this approach has been demonstrated for patients with metastatic colorectal cancer (*22,23*). In patients with colorectal metastases to the liver, the objective response of tumors to 5-FU (*22*) and survival in the years after treatment with 5-FU (*21*) were reliably correlated with SUVs for tumor uptake of ^{18}F-FU determined with PET. An SUV of >3.0 was associated with regression of tumor in the months after therapy, as assessed by serial CT scans, and with survival in every case that exceeded 1.75 y after therapy; an SUV of <1.2 was associated in all cases with tumor progression and survival in all

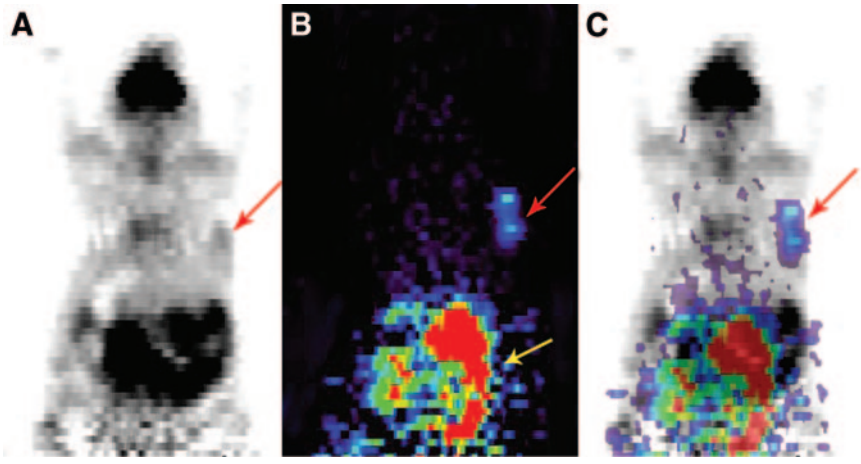

FIGURE 3. Whole-body microPET images of MCF-7 tumor from MCF-7 cells subcutaneously injected into right shoulder. (A and B) Representative tomographic coronal slices of tumor (indicated by red arrow) in same mouse imaged after 1 h of uptake of ~9 MBq of ^{18}F-FDG (A) and after 30 min of uptake of ~9 MBq of ^{18}F-FPAC (B) injected via tail vein. Yellow arrow indicates that most ^{18}F-FPAC biodistribution occurs in abdominal and pelvic areas, related to excretion. Animals were imaged prone such that left side of image corresponds to left side of animal. (C) Fused ^{18}F-FDG and ^{18}F-FPAC images.

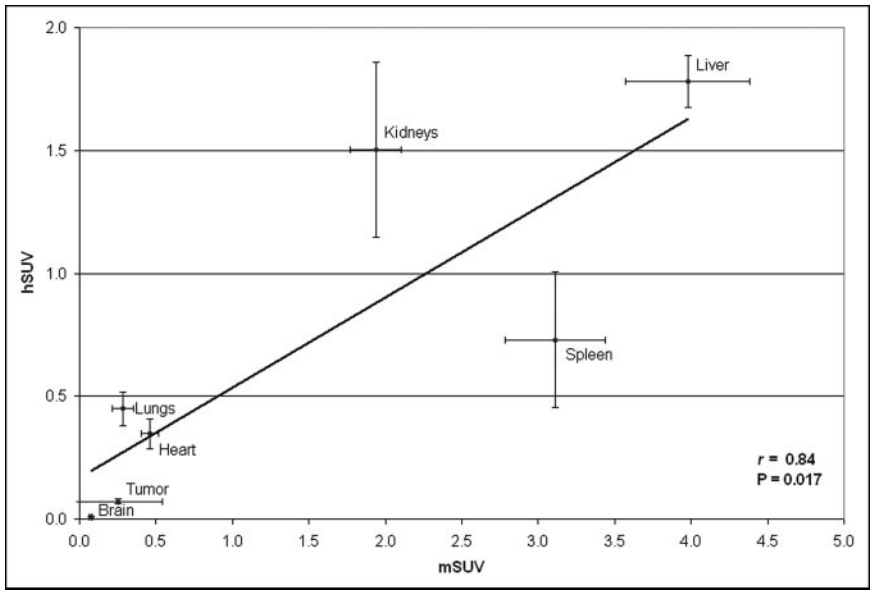

FIGURE 4. Comparison of hSUVs and mSUVs of ^{18}F-FPAC in female athymic mice bearing MCF-7 tumors. Error bars indicate SEM.

cases of less than 1 y. Patients having tumors with intermediate SUVs experienced an intermediate mean response.

One third of breast cancer patients have histologic evidence of axillary lymph node metastases at the time of diagnosis; these women will virtually all be prescribed some regimen of pharmacotherapy, yet 30% of them will experience relapse and nearly 60% will die of this disease within the ensuing 15 y (*24*). As a consequence, much attention has been paid to developing more effective strategies for predicting chemotherapy resistance in advance of administration of those toxic compounds.

This study confirms that ^{18}F-FPAC biodistribution provides a good estimate of PAC biodistribution. The distribution of the tracer was related mainly to the metabolism and excretion routes reported for the parental drug, PAC. Moreover, the biodistribution of ^{18}F-FPAC closely paralleled that of the parental drug, PAC, as assessed by comparison with ^{3}H-PAC biodistribution, and was affected little by the coadministration of more pharmacologic doses of unlabeled PAC. This finding is not surprising, because the uptake of PAC is not receptor driven and, therefore, likely is not saturable but nonetheless needs to be empirically established. microPET imaging data correlated well with uptake data determined by organ harvesting.

The expression of the multidrug resistance gene (MDR-1), which codes for a P-gp efflux pump, has been shown to play a major role in the resistance of cancers to PAC treatment (*25,26*) but is not the sole cause of chemoresistance (*27*). For example, taxane resistance is also affected by the ability of the drug to reach its tumoral target. P-gp is

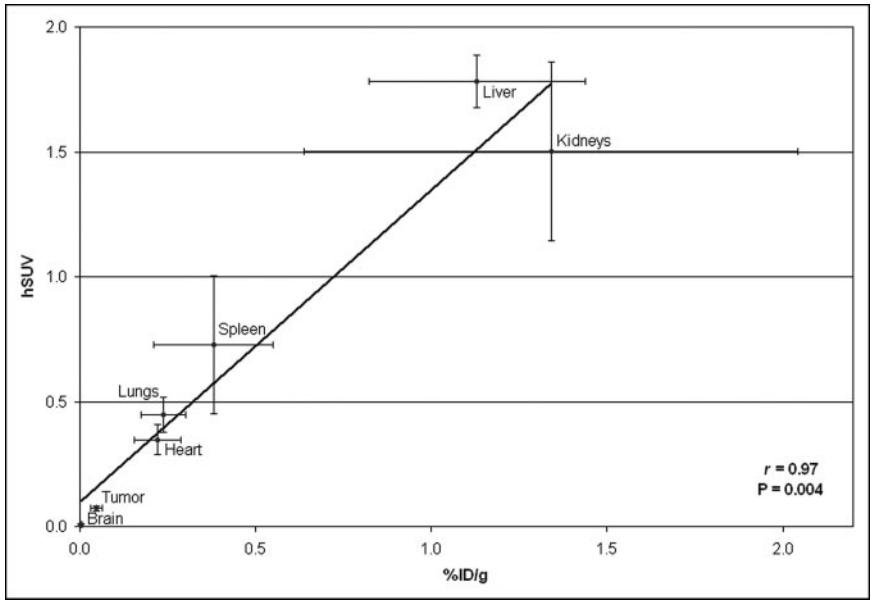

FIGURE 5. Comparison of hSUVs and %ID/g units of ^{18}F-FPAC in female athymic mice bearing MCF-7 tumors. Each point represents mean of determinations from 22 mice. Error bars indicate SEM.

expressed in many organs, including the lungs, brain, and liver (*28,29*), although little is known about the correlation between relative concentrations and corresponding activities of P-gp in those tissues. Our results show that pretreatment with the P-gp modulator cyclosporine tended to double the tumor uptake of both ^{3}H-PAC and ^{18}F-FPAC, consistent with recently reported observations; the effect of genetically knocking out P-gp activity on ^{18}F-FPAC uptake, as determined by organ harvesting, was examined previously (*16,17*).

CONCLUSION

Our PET data indicate that ^{18}F-FPAC holds promise for the noninvasive quantification of PAC distribution in vivo and for predicting subsequent resistance to PAC chemotherapy of breast cancer. Studies such as this one may help to lay the groundwork needed to better use image-guided approaches in the treatment of breast cancer patients—and particularly in the avoidance of chemotherapeutic regimens less likely to be effective because of various mechanisms of physiologic resistance.

ACKNOWLEDGMENTS

The authors acknowledge the faculty and staff in the cyclotron and microPET facilities, including the valuable assistance of Dr. Nagichettiar Satyamurthy, Dr. Arion Chatziioannou, Dr. David Stout, Dr. Waldemar Ladno, and Judy Edwards. Special thanks are due to Christine Dy, Vahe Azarian, and Cheryl Poepping for their technical help as well as to Goran Lacan for useful discussions. We also acknowledge the help and support of the staff at the Ahmanson Biological Imaging Center Nuclear Medicine Clinic. We are grateful to Dr. William Eckelman for his critical input and for the invaluable support that he and his laboratory staff provided in the radiosynthesis of ^{18}F-FPAC. This study was supported by a postdoctoral scholarship from the Fonds de la Recherche en Santé du Québec, by an NIH Research Training in Pharmacological Sciences training grant, and by the University of California Research Mentorship Program. This project also was supported by the California Breast Cancer Research Program.

REFERENCES

1. Jemal A, Murray T, Samuels A, Ghafoor A, Ward E, Thun MJ. Cancer statistics. *CA Cancer J Clin*. 2003;53:5–26.
2. Von Hoff DD, Weisenthal L. In vitro methods to predict patient response to chemotherapy. *Adv Pharmacol Chemother*. 1980;17:133–156.
3. Robert NJ, Martin L, Taylor CD, et al. Nuclear binding of the estrogen receptor: a potential predictor for hormone response in metastatic breast cancer. *Breast Cancer Res Treat*. 1990;16:273–278.
4. Volm M, Efferth T. Relationship of DNA ploidy to chemoresistance of tumors as measured by in vitro tests. *Cytometry*. 1990;11:406–410.
5. Jarvinen TA, Holli K, Kuukasjarvi T, Isola JJ. Predictive value of topoisomerase II alpha and other prognostic factors for epirubicin chemotherapy in advanced breast cancer. *Br J Cancer*. 1998;77:2267–2273.
6. Pegram MD, Pauletti G, Slamon DJ. HER-2/neu as a predictive marker of response to breast cancer therapy. *Breast Cancer Res Treat*. 1998;52:65–77.
7. Nishimura R, Nagao K, Miyayama H, et al. Thymidylate synthase levels as a therapeutic and prognostic predictor in breast cancer. *Anticancer Res*. 1999;19:5621–5626.
8. Sjostrom J, Blomqvist C, Heikkila P, et al. Predictive value of p53, mdm-2, p21 and mib-1 for chemotherapy response in advanced breast cancer. *Clin Cancer Res*. 2000;6:3103–3110.
9. Metzger R, Deglmann CJ, Hoerrlein S, Zapf S, Hilfrich J. Toward in-vitro prediction of an in-vivo cytostatic response of human tumor cells with a fast chemosensitivity assay. *Toxicology*. 2001;166:97–108.
10. Goh LB, Spears KJ, Yao D, et al. Endogenous drug transporters in in vitro and in vivo models for the prediction of drug disposition in man. *Biochem Pharmacol*. 2002;64:1569–1578.
11. Sladek NE, Kollander R, Sreerama L, Kiang DT. Cellular levels of aldehyde dehydrogenases (ALDH1A1 and ALDH3A1) as predictors of therapeutic responses to cyclophosphamide-based chemotherapy of breast cancer: a retrospective study—rational individualization of oxazaphosphorine-based cancer chemotherapeutic regimens. *Cancer Chemother Pharmacol*. 2002;49:309–321.
12. Li C, Yu DF, Inoue T, et al. Synthesis, biodistribution and imaging properties of indium-111-DTPA-paclitaxel in mice bearing mammary tumors. *J Nucl Med*. 1997;38:1042–1047.
13. Brady F, Luthra SK, Brown GD, et al. Radiolabelled tracers and anticancer drugs for assessment of therapeutic efficacy using PET. *Curr Pharm Des*. 2001;7:1863–1892.
14. Horwitz SB. Mechanism of action of taxol. *Trends Pharmacol Sci*. 1992;13:134–136.
15. Kiesewetter DO, Eckelman WC. Radiochemical synthesis of [^{18}F]fluoropaclitaxel ([^{18}F]FPAC) [abstract]. *J Labelled Compds Radiopharm*. 2002;44(suppl):S903–S905.
16. Kiesewetter DO, Jagoda EM, Kao CH, et al. Fluoro-, bromo-, and iodopaclitaxel derivatives: synthesis and biological evaluation. *Nucl Med Biol*. 2003;30:11–24.
17. Kurdziel KA, Kiesewetter DO, Carson RE, Eckelman WC, Herscovitch P. Biodistribution, radiation dose estimates, and in vivo Pgp modulation studies of ^{18}F-paclitaxel in nonhuman primates. *J Nucl Med*. 2003;44:1330–1339.
18. Li C, Newman RA, Wu QP, et al. Biodistribution of paclitaxel and poly(L-glutamic acid)-paclitaxel conjugate in mice with ovarian OCa-1 tumor. *Cancer Chemother Pharmacol*. 2000;46:416–422.
19. Lavie Y, Cao H, Volner A, et al. Agents that reverse multidrug resistance, tamoxifen, verapamil, and cyclosporin A, block glycosphingolipid metabolism by inhibiting ceramide glycosylation in human cancer cells. *J Biol Chem*. 1997;272:1682–1687.
20. Gottesman MM, Fojo T, Bates SE. Multidrug resistance in cancer: role of ATP-dependent transporters. *Nat Rev Cancer*. 2002;2:48–58.
21. Stahl A, Wider H, Piert M, Wester HJ, Senekowitsch-Schmidtke R, Schwaiger M. Positron emission tomography as a tool for translational research in oncology. *Mol Imaging Biol*. 2004;6:214–224.
22. Dimitrakopoulou-Strauss A, Strauss LG, Schlag P, et al. Fluorine-18-fluorouracil to predict therapy response in liver metastases from colorectal carcinoma. *J Nucl Med*. 1998;39:1197–1202.
23. Moehler M, Dimitrakopoulou-Strauss A, Gutzler F, Raeth U, Strauss LG, Stremmel W. ^{18}F-Labeled fluorouracil positron emission tomography and the prognoses of colorectal carcinoma patients with metastases to the liver treated with 5-fluorouracil. *Cancer*. 1998;83:245–253.
24. Bonadonna G. Evolving concepts in the systemic adjuvant treatment of breast cancer. *Cancer Res*. 1992;52:2127–2137.
25. Mimnaugh EG, Fairchild CR, Fruehauf JP, Sinha BK. Biochemical and pharmacological characterization of MCF-7 drug-sensitive and AdrR multidrug-resistant human breast tumor xenografts in athymic nude mice. *Biochem Pharmacol*. 1991;42:391–402.
26. Orr GA, Verdier-Pinard P, McDaid H, Horwitz SB. Mechanisms of taxol resistance related to microtubules. *Oncogene*. 2003;22:7280–7295.
27. Yu D, Liu B, Tan M, Li J, Wang SS, Hung MC. Overexpression of c-erbB-2/neu in breast cancer cells confers increased resistance to taxol via mdr-1-independent mechanisms. *Oncogene*. 1996;13:1359–1365.
28. Schrenk D, Michalke A, Gant TW, Brown PC, Silverman JA, Thorgeirsson SS. Multidrug resistance gene expression in rodents and rodent hepatocytes treated with mitoxantrone. *Biochem Pharmacol*. 1996;52:1453–1460.
29. Beaulieu E, Demeule M, Ghitescu L, Beliveau R. P-Glycoprotein is strongly expressed in the luminal membranes of the endothelium of blood vessels in the brain. *Biochem J*. 1997;326:539–544.

JNM The Journal of NUCLEAR MEDICINE

Estimation of Paclitaxel Biodistribution and Uptake in Human-Derived Xenografts In Vivo with ^{18}F-Fluoropaclitaxel

Anne Gangloff, Wei-Ann Hsueh, Amanda L. Kesner, Dale O. Kiesewetter, Betty S. Pio, Mark D. Pegram, Malgorzata Beryt, Allison Townsend, Johannes Czernin, Michael E. Phelps and Daniel H.S. Silverman

J Nucl Med. 2005;46:1866-1871.

The Journal of Nuclear Medicine is published monthly.
SNMMI | Society of Nuclear Medicine and Molecular Imaging
1850 Samuel Morse Drive, Reston, VA 20190.
(Print ISSN: 0161-5505, Online ISSN: 2159-662X)

SNMMI SOCIETY OF NUCLEAR MEDICINE AND MOLECULAR IMAGING